Vibrationally induced nuclear quadrupole coupling in the $v_3=1$ state of $^{189}OsO_4$

Flavio Scappini,[a] Welf A. Kreiner,[b] Joan M. Frye,[c] and Takeshi Oka
Department of Chemistry and Department of Astronomy and Astrophysics, The University of Chicago, Chicago, Illinois 60637

(Received 24 March 1987; accepted 6 August 1987)

Electric nuclear quadrupole hyperfine structure arising from a quadrupolar nucleus at the center of tetrahedral molecules, such as $^{189}OsO_4$, is symmetry forbidden. However, through vibration–rotation distortion a small nuclear quadrupole coupling is induced. The hyperfine structure due to the vibrationally induced eqQ has been measured for a number of P- and R-branch transitions in the ν_3 fundamental of $^{189}OsO_4$, by using inverse Lamb dip spectroscopy. Microwave modulation sidebands of CO_2 laser lines have been used as the tunable infrared radiation. From the analysis of the observed hyperfine structure patterns, the values of the scalar and tensor coupling constants have been determined to be $\chi_s^V = -4.103 \pm 0.048$ MHz and $\chi_t^V = -3.090 \pm 0.059$ MHz.

I. INTRODUCTION

A tetrahedral molecule such as $^{189}OsO_4$ having a central atom with an electric nuclear quadrupole moment ($I = 3/2$) does not show nuclear quadrupole hyperfine structure in the ground rovibronic state because of the high electronic symmetry. However, in vibrationally excited state with degeneracy, this symmetry is broken and a small electric quadrupole coupling is produced. The order of magnitude of the resultant quadrupole coupling constant eqQ is smaller than the ordinary values of eqQ by a factor of κ^2, where κ is the Born–Oppenheimer constant [expressed in terms of the electron mass m and the nuclear mass M as $\kappa = (m/M)^{1/4}$].

The quadrupole hyperfine structure in the infrared rovibrational spectrum of $^{189}OsO_4$ arising from such quadrupole coupling was first reported by Letokhov and his colleagues[1–3] in their sub-Doppler spectroscopy of OsO_4 using the accidental coincidences between CO_2 laser lines within their narrow (~ 30 MHz) tuning range and the ν_3 band lines of OsO_4. The transitions reported by them are most probably hot bands and assignment has not been possible so far, even after the extensive analysis of the ν_3 band by McDowell and others[4] in 1978. Some unassignable hyperfine structure has also been observed in infrared–radio frequency double resonance experiments of OsO_4.[5]

Later, Bordé *et al.*,[6] by using a high pressure CO_2 waveguide laser, succeeded in observing three hyperfine patterns of $^{189}OsO_4$. Hougen and Oka[7] developed a theory on the vibrationally induced nuclear quadrupole coupling in tetrahedral and octahedral molecules and applied it to the analysis of the hyperfine patterns observed by Bordé *et al.*[6] This theory gave the scalar quadrupole coupling constant χ_s^V and the tensor quadrupole coupling constant χ_t^V, as $\chi_s^V = -4.29 \pm 0.17$ MHz and $\chi_t^V = -3.14 \pm 0.23$ MHz, respectively.

Subsequently, Palma and Bordé[8] developed a theoretical treatment for the rotation induced quadrupole coupling and applied it to $^{189}OsO_4$. Recently, Bordé *et al.*[9] succeeded in measuring the rotational induced χ_s^R and χ_t^R in the ground state.

The present investigation is aimed at gathering more experimental data on this problem. Two out of the three quadrupole hyperfine patterns observed by Bordé *et al.*[6] belong to a pair of very close components of a manifold. Thus, in Hougen and Oka's treatment,[7] two constants were determined from two independent patterns. The more extensive spectrum to be obtained in this work will be useful to check the validity of their analysis and to refine their results.

II. EXPERIMENTAL

The spectrometer used has been described in detail elsewhere.[10,11] Only a brief description is given here. It consists of a continuous flow CO_2 laser, whose radiation (~ 3 W) is mixed in a CdTe crystal with 12–18 GHz synthesized microwave radiation after power amplification (~ 20 W). Frequency sidebands are generated at $\nu_{CO_2} \pm \nu_{MW}$, with the power of $\gtrsim 0.5$ mW. The corresponding power density in a beam of ~ 6 mm diameter is sufficient to allow saturation spectroscopy on OsO_4 at a few mTorr pressure. The laser itself is locked to the zero of the first derivative of the 4.3 μm CO_2 fluorescence Doppler profile, using a Lansing Model 80.215 lock-in stabilizer.

The microwave radiation was frequency modulated at 10 kHz and the signal was phase sensitive detected at twice the modulation frequency. The accuracy of absolute frequency measurements is estimated to be ± 2 MHz, while that of the splittings is only dependent on the short term laser stability and it is a few percent ($\sim 5\%$) of the splittings.

The spectra were taken using commercial OsO_4 from Matheson, Coleman, and Bell Manufacturing Chemists, Ohio. The natural abundance of the ^{189}Os isotope is 16.1%. A small amount of $^{189}OsO_4$ was prepared starting from ^{189}Os at 99.5%, supplied by Oak Ridge National Laboratory, Tenn. The preparation was carried out according to Ref. 12.

[a] Permanent address: Instituto di Spettroscopia Molecolare del C.N.R., Via De'Castagnoli 1, 40126 Bologna, Italy.
[b] Permanant address: Abteilung Für Physikalische Chemie, Universität Ulm, Oberer Eselsberg, D-7900 Ulm, West Germany.
[c] Present address: Department of Chemistry, Brookhaven National Laboratory, Upton, New York 11973.

 0021-9606/87/225644-05$02.10

This latter sample was used only to check lines in cases where ambiguities in the spectra of OsO_4 occurred.

III. FINE STRUCTURE IN THE ν_3 BAND OF OsO_4

The infrared-active stretching fundamental $\nu_3(F_2)$ band of OsO_4 at 961 cm^{-1} coincides with the 00°1–[10°0–02°0]$_1$ CO_2 laser transitions in the 10.4 μm region. This band, which has been investigated by McDowell *et al.*[4] using a Michelson interferometer and a tunable semiconductor diode laser, satisfies the symmetry requirements to induce a vibrational quadrupole coupling and is suitable to be studied with the CO_2 sideband laser spectrometer.

In a triply degenerate vibrational state of a tetrahedral molecule, the vibrationally induced angular momentum l couples with the pure rotational angular momentum **R** to give the resultant total angular momentum **J**. For the first excited vibrational state of a triply degenerate vibration, therefore, a given J level splits into three Coriolis sublevels ($R = J+1, J, J-1$). Each Coriolis sublevel further splits into its tetrahedral fine structure by higher order vibration–rotation interactions. Each rovibrational state is thus labeled by two quantum members J and R and one of the symmetry species A_1, A_2, E, F_1, F_2. Throughout the paper the symmetry designation according to Dorney and Watson[13] will be followed.

The selection rules for the rovibrational electric dipole transitions are $\Delta J = 0, \pm 1, \Delta R = 0$, together with $A_1 \leftrightarrow A_2$, $E \leftrightarrow E$, $F_1 \leftrightarrow F_2$.

In the case of OsO_4, since the spin of the identical nuclei is zero, only levels with A_1 or A_2 symmetry can occur.

IV. HYPERFINE STRUCTURE

A tetrahedral molecule, containing a central quadrupolar nucleus, has a vibrational and centrifugal distortion induced quadrupole coupling, which can be described by an effective first order Hamiltonian of the form

$$H_Q = H_Q^V + H_Q^R , \tag{1}$$

where H_Q^V is the effective vibrational quadrupole coupling operator with nonvanishing matrix elements only for E and F_2 symmetry vibrational states. The analytical expressions for H_Q^V are given in Ref. 7 by the Eqs. (19) and (20) for a triply and a doubly degenerate vibration, respectively. The H_Q^R term is the effective operator for the centrifugal distortion contribution which has nonvanishing matrix elements even in the ground vibrational state. The analytical expression for H_Q^R is given in Ref. 8 by Eq. (11).

The quadrupole coupling energy is

$$W_Q = -eqQ(J,R,\kappa) \cdot Y(I,J,F) , \tag{2}$$

where $eqQ(J,R,\kappa)$ is the effective quadrupole coupling constant for the particular rovibrational state considered (κ designates the symmetry species) and is composed of a vibrational and a centrifugal distortion part; $Y(I,J,F)$ is the Casimir function.

The effective $eqQ(J,R,\kappa)$ can be expressed in terms of four rotational-state-independent parameters: χ_s^V and χ_t^V accounting for the vibrational dependence, and χ_s^R and χ_t^R accounting for the rotational dependence. The relationships are given by Eqs. (26) of Ref. 7 and Eqs. (16) of Ref. 8.

For $^{189}OsO_4$ the rotational contribution to the hyperfine splittings of the ν_3 state is significant for high rotational levels. However, since the observed $\Delta R = 0$ rovibrational selection rule takes the difference between the hyperfine level structures in the excited state and in the ground state, the rotation contribution to the hyperfine spectrum is reduced to be on the order of our experimental accuracy. We, therefore, consider only χ_s^V and χ_t^V.

As an example the hyperfine splitting of the rovibrational $J = 30, R = 31, A_1^{(3)}$ level is shown in Fig. 1, for positive eqQ. In addition to the hyperfine structure due to the electric quadrupole moment of the nucleus, the interaction of the nuclear magnetic moment with rotation and vibration produces observable energy shifts,[6] which are expressed as

$$W_{SRV} = -\tfrac{1}{2}[F(F+1) - J(J+1) - I(I+1)] \times \{C + \frac{A}{2J(J+1)}[R(R+1) - J(J+1) - l(l+1)]\} . \tag{3}$$

This energy contribution does not affect the center of the doublets, shown in Fig. 1, but only changes their relative splittings.

V. RESULTS AND DISCUSSION

A. Unperturbed levels

The infrared transitions of $^{189}OsO_4$ were searched for using the predictions based upon the ν_3 spectroscopic constants of Ref. 4. A number of P- and R- branch rovibrational

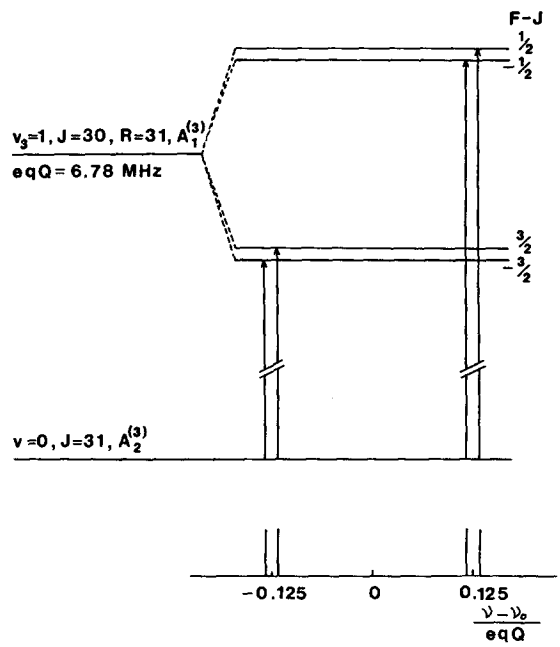

FIG. 1. Calculated splitting of the $J = 30$, $R = 31$, $A_1^{(3)}$ rotational level in the $v_3 = 1$ state of $^{189}OsO_4$ due to the vibrational induced nuclear quadrupole coupling and hyperfine structure $\Delta F = \pm 1$ of the corresponding $\nu_3 P(31)$ $A_2^{(3)}$ rovibrational transition. The observed eqQ (30, 31, $A_1^{(3)}$) is 6.78 MHz. The ground state centrifugal distortion hyperfine splitting is neglected.

transitions were observed as doublets with a FWHM of each line of ~200 kHz. The resolution of the spectrometer at the time of the experiment was not sufficient in most cases, to further resolving each component of the doublet.

An example of hyperfine spectrum corresponding to the five $P(31)$ transitions is given in Fig. 2. The splitting between the centers of the two $|J-F|=\frac{3}{2}$ and $|J-F|=\frac{1}{2}$ components decreases in going from the C_{3v} to the D_{2d} extreme in the tetrahedral fine structure levels of the $J=30$, $R=31$ Coriolis sublevel. The dependence of $eqQ\,(30,31,\kappa)$ on the tetrahedral splitting is shown in Fig. 3. A case where the hyperfine splitting is comparable to the tetrahedral splitting is shown in Fig. 4 for the two transitions $\nu_3R(24)\,A_2^{(2)}$ and $\nu_3R(24)\,A_1^{(3)}$. Here, the quartet feature of each rovibrational transition is completely resolved, as shown in Fig. 5. It would have been nice to observe the Q-branch transitions of $^{189}OsO_4$ which occur as a great many lines near 961 cm^{-1}, but, since the closest CO_2 laser line is $R(0)$, the infrared

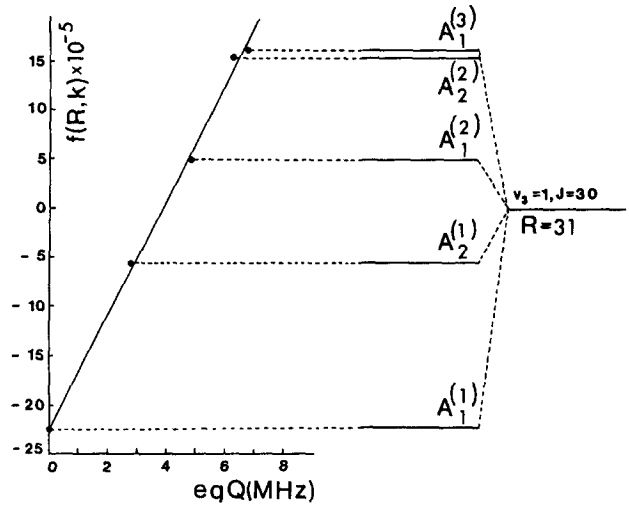

FIG. 3. Plot of the $eqQ\,(30,31,\kappa)$ observed values, for $^{189}OsO_4$ in the $v_3=1$ state, against the splitting function $f(R,\kappa)$, which is proportional to the tetrahedral splitting energy of the $J=30$, $R=31$ Coriolis sublevel. The symmetries refer to the excited state.

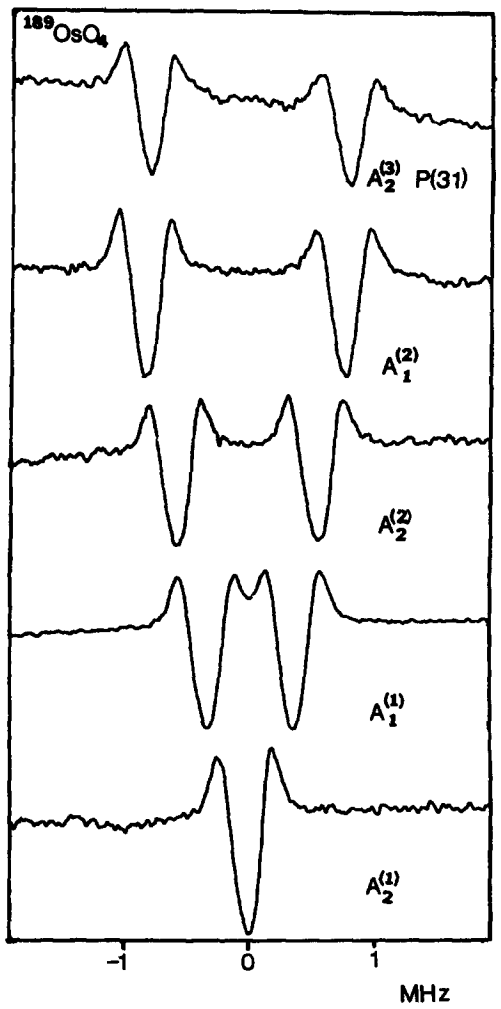

FIG. 2. Hyperfine splitting of the five $\nu_3P(31)$ rovibrational transitions of $^{189}OsO_4$ showing the characteristic decrease in going from the C_{3v} to the D_{2d} extreme in the tetrahedral fine structure levels of the $J=30$, $R=31$ Coriolis sublevel. The symmetries refer to the ground state. $^{189}OsO_4$ is in natural abundance. The lower sideband of the CO_2 $10P(8)$ laser line is swept around the center of each doublet. The time cosntant is 1 s. The microwave frequency modulation is 10 kHz and the signal is displayed in the second derivative mode.

power was not sufficient to produce saturating sideband power. The 961 cm^{-1} frequency can be more efficiently produced either using CO_2 isotopes or a N_2O laser. The hyperfine structure of the Q-branch transitions would be particularly interesting because it is not affected by the magnetic spin–rotation–vibration coupling and, moreover, the quadrupole coupling constant is twice as large (with opposite sign) as for P and R branches, for a given R and κ.[7]

The measured hyperfine splittings together with the rovibrational transition frequencies are presented in Table I. Using the expression (2) the $eqQ(J,R,\kappa)$ values (observed values) of Table II are derived. A comparison of these values with those which can be predicted from the already existing χ_s^V and χ_t^V values,[7] showed a fair agreement for most of the measured transitions and quite large discrepancies for some of them. These last ones are listed separately in Tables I and

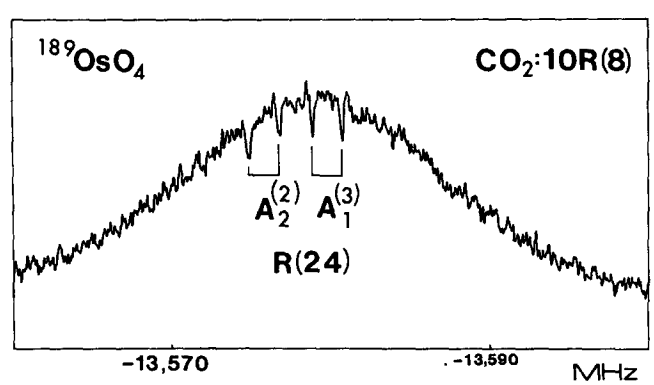

FIG. 4. Doppler-broadened profile of $R(24)\,A_2^{(2)}$ and $R(24)\,A_1^{(3)}$ rovibrational transitions in the ν_3 band of $^{189}OsO_4$. The quadrupole hyperfine splitting is comparable, in this case, with the tetrahedral splitting at the C_{3v} limit. The symmetries refer to the ground state. $^{189}OsO_4$ is in natural abundance. The time constant is 0.1 s. The microwave frequency modulation is 10 kHz and the signal is displayed in the second derivative mode. The CO_2 laser oscillates at 10 $R(8)$ and the microwave frequency is indicated on abscissa.

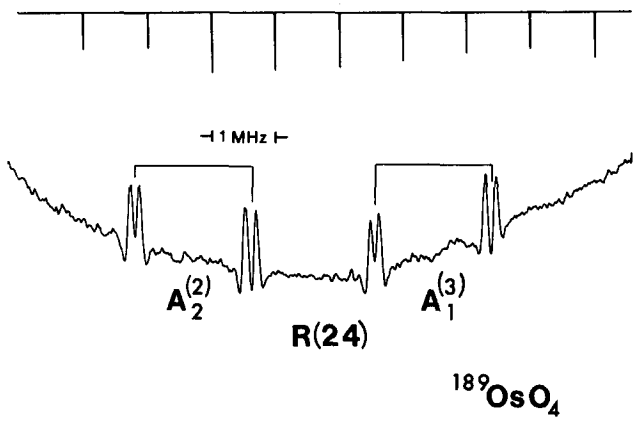

FIG. 5. Same as Fig. 4, showing the multiplet structure on an expanded scale. The time constant is 1 s.

II under "perturbed transitions" and were not used in the calculation.

The two rotational-state-independent quantities χ_s^V and χ_t^V were least-squares fitted to the $eqQ(J,R,\kappa)$ values, from the nonperturbed transitions, and the results are given in Table II. Using these quantities the $eqQ(J,R,\kappa)$ values for all the measured transitions were recalculated and they are presented in the last column of Table II. The calculated $eqQ(J,R,\kappa)$ values, for the nonperturbed transitions, reproduce the observed splittings within their quoted experimental errors and with a standard deviation of 27 kHz. Finally, the $(A-C)$ value could also be determined from the two resolved quartet spectra of Fig. 5 and the result is given in Table II.

TABLE I. Measured rovibrational transitions in the ν_3 band of $^{189}OsO_4$ and hyperfine structure splittings.

Transition[a]		Observed frequency (MHz)	Obs. − calc.[b] frequency (MHz)	Observed[c] hyperfine splitting (kHz)
$R(11)$	A_2	28 908 916 (2)	14	1038 (20)
$R(17)$	A_2	28 950 159 (2)	2	1325 (74)
	A_1	28 950 282 (2)	−6	683 (51)
$R(22)$	$A_1^{(2)}$	28 984 166 (2)	15	1614 (99)
$R(24)$	$A_1^{(3)}$	28 997 554 (2)	−31	1725 (81)
	$A_2^{(2)}$	28 997 558 (2)	−31	1827 (55)
	$A_1^{(2)}$	28 997 776 (2)	−31	1298 (56)
R(26)	$A_1^{(2)}$[d]	29 011 181	−46	1505
$P(20)$	$A_1^{(2)}$	28 681 578 (2)	−30	1289 (86)
	$A_2^{(1)}$	28 681 715 (2)	−32	770 (57)
	$A_1^{(1)}$	28 682 021 (2)	−37	−467 (31)
$P(31)$	$A_2^{(3)}$	28 600 502 (2)	−33	1696 (27)
	$A_1^{(2)}$	28 600 522 (2)	−33	1562 (88)
	$A_2^{(2)}$	28 600 807 (2)	−33	1196 (20)
	$A_1^{(1)}$	28 601 097 (2)	−37	682 (17)
	$A_2^{(1)}$	28 601 538 (2)	−43	0
$P(49)$	$A_2^{(4)}$[d]	28 464 739	0	1862
	$A_1^{(4)}$[d]	28 464 742	1	1860
		Perturbed transitions		
$R(30)$	$A_2^{(3)}$	29 037 759 (2)	−77	409 (10)
	$A_1^{(3)}$	29 037 808 (2)	−30	1650 (30)
	$A_2^{(2)}$	29 038 291 (2)	10	552 (41)
$R(43)$	$A_1^{(3)}$	29 123 735 (2)	23	641 (59)
	$A_2^{(4)}$	29 123 781 (2)	66	1507 (41)
$R(49)$	$A_1^{(4)}$	29 162 551 (2)	−28	1552 (29)
	$A_2^{(4)}$	29 162 645 (2)	64	602 (12)
	$A_2^{(3)}$	29 163 029 (2)	56	1212 (25)

[a] The symmetry species refers to the ground state level.
[b] The calculated transition frequencies are based on the ν_3 spectroscopic constants form Ref. 4.
[c] The hyperfine splitting is measured as the difference between the frequencies of the $|F-J|=3/2$ and the $|F-J|=1/2$ unresolved doublets.
[d] From Ref. 6.

TABLE II. Observed and calculated effective nuclear quadrupole coupling constants for $^{189}OsO_4$ in the $v_3=1$ vibrational state. Least-squares fitted values of χ_s^V and χ_t^V.[a]

$v_3=1, J, R, \kappa$	Observed eqQ (MHz)	Calculated[b] eqQ (MHz)
12, 11, A_1	4.15	4.08
18, 17, A_1	5.30	5.25
A_2	2.73	2.90
23, 22, $A_2^{(2)}$	6.45	6.27
25, 24, $A_2^{(3)}$	6.90	7.31
$A_1^{(2)}$	7.31	7.27
$A_2^{(2)}$	5.19	5.09
27, 26, $A_2^{(2)}$[c]	6.02	5.80
19, 20, $A_2^{(2)}$	5.16	5.35
$A_1^{(1)}$	3.08	3.17
$A_2^{(1)}$	−1.87	−1.92
30, 31, $A_1^{(3)}$	6.78	6.73
$A_2^{(2)}$	6.25	6.62
$A_1^{(2)}$	4.78	4.76
$A_2^{(1)}$	2.73	2.89
$A_1^{(1)}$	0.00	0.08
48, 49, $A_1^{(4)}$[c]	7.45	7.20
$A_2^{(4)}$[c]	7.44	7.20
Perturbed transitions		
31, 30, $A_1^{(3)}$	1.64	7.43
$A_2^{(3)}$	6.60	7.44
$A_1^{(2)}$	2.20	6.35
44, 43, $A_2^{(3)}$	2.58	6.88
$A_1^{(4)}$	6.03	7.64
50, 49, $A_2^{(4)}$	6.21	7.02
$A_1^{(4)}$	2.41	7.02
$A_1^{(3)}$	4.85	5.73
$\chi_s^V = -4.103 \pm 0.048$ MHz		
$\chi_t^V = -3.090 \pm 0.059$ MHz		
$(A-C) = 17 \pm 4$ kHz		

[a] The eqQ (J,R,κ) values are listed in this table in the same order as the splittings in Table I. The symmetry species refers to the excited state level.
[b] Calculated using the values of χ_s^V and χ_t^V reported in this table and the expressions (26) of Ref. 7.
[c] From Ref. 6.

B. Perturbed levels

The transitions which show anomalous $eqQ(J,R,\kappa)$ values, see Table II, have the following common features. They all have high J values. The $eqQ(J,R,\kappa)$ observed values, second column in Table II, are always smaller than the calculated ones, third column. In cases of predicted close pairs of transitions, as, e.g., $R(49)$ $A_2^{(4)}$ and $R(49)$ $A_1^{(4)}$, not only the eqQ values are different from those calculated, $\Delta eqQ(50, 49, A_1^{(4)}) = -4.61$ MHz and $\Delta eqQ(50, 49,$

$A_2^{(4)}) = -0.81$ MHz, but also they are widely different from each other, $eqQ(50, 49, A_1^{(4)}) = 2.41$ MHz and $eqQ(50, 49, A_2^{(4)}) = 6.21$ MHz, contrary to the expectation that all states within a C_{3v} manifold should have nearly the same quadrupole coupling constant. In the above example the experimental transition frequencies differ from the calculated ones by 64 and -29 MHz and the lines intensity ratio is 1:3, respectively.

The consideration of the above points leads to thinking that some perturbation occurs which affects the tetrahedral fine structure of these levels. Recently Bordé[14] pointed to us that such perturbation is unlikely and that the discrepancy might be due to misassignment of the transitions.

VI. CONCLUSIONS

The present investigation has provided extensive experimental material to confirm the validity of the Hougen and Oka's theory of quadrupole coupling in tetrahedral molecules.[7] The vibrationally induced quadrupole constants χ_s^V and χ_t^V have been better determined by a least-squares fit to 18 experimental $eqQ(J,R,\kappa)$ values, including those from Ref. 6. Since for the observed spectra the rotational effect cancels almost completely, the only two determined constants χ_s^V and χ_t^V, with the neglect of χ_s^R and χ_t^R, can account for the measured splittings in the ν_3 band within our experimental accuracy. The $(A-C)$ magnetic spin–rotation–vibration contribution has also been measured and it agrees with that obtained in Refs. 6 and 9, within the quoted uncertainties.

Further experimental work on $^{189}OsO_4$ might be directed to obtain spectra of the Q-branch transitions providing useful additional data, as already discussed. Recently, radio-frequency-infrared double resonance experiments were performed, pumping between two close A_1 and A_2 levels in a C_{3v} manifold and observing the corresponding infrared transition. They provided very accurate measurements of the fine tetrahedral splittings.[15]

The importance of high resolution spectroscopy on $^{189}OsO_4$ is not only limited to the fundamental aspects of understanding the fine and hyperfine interactions, but also has a practical impact in connection with laser-induced chemistry, particularly the laser isotope separation.

Finally, the microwave modulation sideband CO_2 laser has proven to be a very powerful tool to do systematic high resolution infrared spectroscopy in the 9–11 μm region. With reference to spherical tops, the present investigation can be extended to other molecules whose vibrational frequencies fall into the tunable frequency range of the laser, as SF_6, RuO_4, etc.

ACKNOWLEDGMENTS

We are grateful to R. S. McDowell for providing us with the calculated spectrum of the ν_3 band of OsO_4, which was essential for our study. We are also grateful to Ch. J. Bordé for some very useful comments. We wish to thank the following institutions: Louis Block Fund of The University of Chicago for financial contribution to this project, NATO and Consiglio Nazionale delle Richerche for support to F. Scappini, Deutsche Forschungsgemeinschaft for support to W. A. Kreiner, National Organization of Black Chemists and Chemical Engineers and Eastman Kodak Company for a grant to J. M. Frye.

[1] Yu. A. Gorokhov, O. N. Kompanets, V. S. Letokhov, G. A. Gerasimov, and Yu. I. Posudin, Opt. Commun. **7**, 320 (1973).
[2] O. N. Kompanets, A. R. Kukudzhanov, V. S. Letokhov, V. G. Minogin, and E. L. Mikhailov, Sov. Phys. JETP **42**, 15 (1976).
[3] E. N. Bazarov, G. A. Gerasimov, K. I. Guryev, V. L. Derbov, M. A. Kovner, Yu. I. Posudin, S. K. Potapov, and V. A. Chenin, J.Quant. Spectrosc. Radiat. Transfer **17**, 7 (1977).
[4] R. S. McDowell, L. J. Radziemski, H. Fliker, H. W. Galbraith, R. C. Kennedy, N. G. Nereson, B. J. Krohn, J. P. Aldridge, J. D. King, and K. Fox, J. Chem. Phys. **69**, 1513 (1978).
[5] P. Glorieux, G. W. Hills, F. Scappini, and T. Oka (unpublished work).
[6] Ch. J. Bordé, M. Ouhayoun, A. Van Lerberghe, C. Salomon, S. Avrillier, C. D. Cantrell, and J. Bordé, in *Laser Spectroscopy IV*, edited by H. Walther and K. W. Rothe (Springer, Berlin, 1979), p. 142.
[7] J. T. Hougen and T. Oka, J. Chem. Phys. **74**, 1830 (1981).
[8] M. L. Palma and J. Bordé, J. Phys. (Paris) **42**, 1239 (1981).
[9] Ch. J. Bordé, J. Bordé, Ch. Breant, Ch. Chardonnet, A. Van Lerberghe, and Ch. Salomon, in *Laser Spectroscopy VII*, edited by T. W. Hänsch and Y. R. Shen (Springer, Berlin, 1985).
[10] G. Magerl, J. M. Frye, W. A. Kreiner, and T. Oka, Appl. Phys. Lett. **42**, 656 (1983).
[11] G. Magerl, W. Schupita, E. Bonek, and W. A. Kreiner, J. Mol. Spectrosc. **83**, 431 (1980).
[12] L. Grube, in *Handbook of Preparative Inorganic Chemistry*, edited by G. Brauer (Academic, New York, 1965), Vol. 2, p. 1603.
[13] A. J. Dorney and J. K. G. Watson, J. Mol. Spectrosc. **42**, 135 (1972).
[14] Ch. J. Bordé (private communication).
[15] F. Scappini, W. A. Kreiner, J. M. Frye, and T. Oka, J. Mol. Spectrosc. **106**, 436 (1984).